

Observation of an Intermediate Tryptophanyl Radical in W306F Mutant DNA Photolyase from *Escherichia coli* Supports Electron Hopping along the Triple Tryptophan Chain[†]

Martin Byrdin,^{*,‡,§} Sandrine Villette,^{‡,§,||} Andre P. M. Eker,[⊥] and Klaus Brettel^{‡,§}

CEA, iBiTecS, Service de Bioénergétique Biologie Structurale et Mécanismes, Gif-sur-Yvette F-91191, France, CNRS, URA 2096, Gif-sur-Yvette F-91191, France, and Department of Cell Biology and Genetics, Medical Genetics Centre, Erasmus University Medical Centre, P.O. Box 2040, 3000 CA Rotterdam, The Netherlands

Received May 11, 2007; Revised Manuscript Received July 3, 2007

ABSTRACT: DNA photolyases repair UV-induced cyclobutane pyrimidine dimers in DNA by photoinduced electron transfer. The redox-active cofactor is FAD in its doubly reduced state FADH[−]. Typically, during enzyme purification, the flavin is oxidized to its singly reduced semiquinone state FADH[•]. The catalytically potent state FADH[−] can be reestablished by so-called photoactivation. Upon photoexcitation, the FADH[•] is reduced by an intrinsic amino acid, the tryptophan W306 in *Escherichia coli* photolyase, which is 15 Å distant. Initially, it has been believed that the electron passes directly from W306 to excited FADH[•], in line with a report that replacement of W306 with redox-inactive phenylalanine (W306F mutant) suppressed the electron transfer to the flavin [Li, Y. F., et al. (1991) *Biochemistry* 30, 6322–6329]. Later it was realized that two more tryptophans (W382 and W359) are located between the flavin and W306; they may mediate the electron transfer from W306 to the flavin either by the superexchange mechanism (where they would enhance the electronic coupling between the flavin and W306 without being oxidized at any time) or as real redox intermediates in a three-step electron hopping process (FADH[•]* ← W382 ← W359 ← W306). Here we reinvestigate the W306F mutant photolyase by transient absorption spectroscopy. We demonstrate that electron transfer does occur upon excitation of FADH[•] and leads to the formation of FADH[−] and a deprotonated tryptophanyl radical, most likely W359[•]. These photoproducts are formed in less than 10 ns and recombine to the dark state in ~1 μs. These results support the electron hopping mechanism.

Photolyase is a flavoprotein that repairs major UV-induced lesions in DNA, the cyclobutane pyrimidine dimers (CPD),¹ by a near-UV to blue-light-induced reaction (for recent reviews, see refs 1 and 2). Most likely, cleavage of the covalent bonds between the two pyrimidines is triggered by electron transfer to the CPD from the excited state of the FAD cofactor in its doubly reduced form (FADH[−]). Isolated photolyase contains the FAD cofactor typically in the singly reduced radical form FADH[•]. However, the latter can be reduced to catalytically active FADH[−] by a distinct photo-reaction called “photoactivation” or “photoreduction”. It can be achieved by visible light (≤680 nm) in the presence of

an extrinsic reductant. The physiological relevance of photoreduction has been questioned recently (3).

According to pioneering work by Heelis, Sancar, and co-workers (reviewed in ref 4), photoreduction of *Escherichia coli* photolyase can be divided into two main steps.

(1) Upon photon absorption, FADH[•] is promoted to an excited state and abstracts an electron from the tryptophan residue W306 [~15 Å from the flavin and exposed to the surface of the protein (5)]. This reaction yields FADH[−] and the W306 cation radical (₃₀₆TrpH^{•+}, where H denotes the N1 proton).

(2) The W306 cation radical is reduced by an extrinsic reductant. This reaction is in competition with back electron transfer from FADH[−] which has a time constant of ~12 ms at pH 7.4 (6).

The mechanism of step 1 has been a matter of some debate. Until recently, it appeared to be established that the initially formed excited state ²FADH[•]* (the superscript number denotes the spin multiplicity) undergoes rapid (~100 ps) intersystem crossing to form a meta-stable quartet state ⁴FADH[•]* (intrinsic lifetime of ~1 μs) and that the latter abstracts an electron from W306 in a single reaction step in ~1 μs (4). Quantum chemical computations confirmed that single-step electron tunneling from W306 to ⁴FADH[•]* could occur in ~1 μs; the calculated tunneling pathway involved

[†] This work was supported by Agence Nationale de la Recherche Grant ANR-05-BLAN-0304-01 and The Netherlands Organization for Scientific Research (NWO-CW 700.51.304).

* To whom correspondence should be addressed. Telephone: (33) 1 69 08 90 14. Fax: (33) 1 69 08 87 17. E-mail: Martin.Byrdin@cea.fr.

[‡] CEA.

[§] CNRS.

^{||} Permanent address: Centre de Biophysique Moléculaire, CNRS UPR 4301, conventionnée avec l'Université d'Orléans, Rue Charles Sadron, 45071 Orléans Cedex 2, France.

[⊥] Erasmus University Medical Centre.

¹ Abbreviations: CPD, cyclobutane pyrimidine dimer; FADH[•], singly reduced neutral radical state of FAD; FADH[−], doubly reduced state of FAD; TrpH, neutral tryptophan; TrpH^{•+}, tryptophan cation radical state (TrpH-e[−]); Trp[•], tryptophan neutral radical state (TrpH-e[−]-H⁺); PCET, proton-coupled electron transfer.

two more tryptophans, W382 and W359 (located between the flavin and W306), as virtual intermediates (7).

Since 2000, we have presented evidence of a different mechanism for step 1, namely stepwise electron hopping through the chain $\text{FADH}^\circ \leftarrow \text{W382} \leftarrow \text{W359} \leftarrow \text{W306}$ (8–10). The transient absorption data obtained strongly suggest that the initial excited state $^2\text{FADH}^{\circ*}$ abstracts an electron from the proximal tryptophan residue W382 in ~ 30 ps, that W306 is oxidized in less than 10 ns (time resolution limit of that experiment), and that ${}_{306}\text{TrpH}^{\circ+}$ releases a proton to the aqueous phase in ~ 200 ns, yielding the neutral radical ${}_{306}\text{Trp}^\circ$ (8). Replacement of either W382 or W359 with phenylalanine essentially blocked photo-oxidation of W306 (9, 10). A tens-of-picoseconds time scale for the reduction of excited FADH° was recently confirmed by Wang et al. (11), although this study revealed some kinetic heterogeneity.

A central piece of evidence in favor of a single-step electron transfer from W306 to $^4\text{FADH}^{\circ*}$ in ~ 1 μs in *E. coli* wild-type photolyase had been obtained in a study of a mutant photolyase in which W306 had been replaced with phenylalanine, an amino acid that is much harder to oxidize than tryptophan. Upon excitation of FADH° , transient absorption revealed a species that decayed to the dark state in ~ 500 ns; this species was identified as the quartet state $^4\text{FADH}^{\circ*}$ (12). Hence, W382 and W359 appeared not to reduce excited FADH° . As this implication contradicts the stepwise electron hopping mechanism suggested by our work, we set out to reexamine the W306F mutant photolyase from *E. coli*. The data presented here demonstrate that photoinduced electron transfer does occur in this mutant and that it leads to a reaction product composed of FADH^- and a deprotonated tryptophanyl radical, most likely ${}_{359}\text{Trp}^\circ$. Our results do not provide any evidence of a long-lived flavin quartet state but strongly support the electron hopping mechanism.

MATERIALS AND METHODS

Mutagenesis. The photolyase W306F mutant was obtained from pKE (13), which is pKK223-3 harboring the *E. coli* wild-type photolyase gene, by the Quick Change mutagenesis method (Stratagene) using GGACGGATCGTGTA-CAGTTTCAGAGCAATCCCGCACATTTACAGG as the primer. The mutated gene was overexpressed in *E. coli* KY29 (14), a photoreactivation deficient strain in which the endogenous photolyase gene has been inactivated by replacement with a chloramphenicol resistance marker (15).

Proteins. After growth at 37 °C in an ampicillin- and chloramphenicol-containing medium, mutant photolyase was induced with isopropyl β -D-thiogalactopyranoside at 27 °C. Cells were destructured by sonication in the presence of 10 mM 2-mercaptoethanol. After centrifugation (twice) at 43000g for 1 h, photolyase was purified by chromatography on heparin-Sepharose C1-6B resin (GE Healthcare Pharmacia) by elution with a 0.1 to 1.1 M NaCl gradient in 0.01 M potassium phosphate (pH 7.0) and 10 mM mercaptoethanol, followed by chromatography on SP-Sepharose fast flow resin (GE Healthcare Pharmacia) eluted with a 0.04 to 0.3 M NaCl gradient. The final preparation was estimated to be $>98\%$ pure. *E. coli* wild-type photolyase was overexpressed and purified as described previously (16).

Sample Preparation and Characterization. Samples were stored at -80 °C in 10 mM phosphate buffer (pH 7.0), also

containing 0.25 M NaCl, 18% (w/w) glycerol, and 5 mM mercaptoethanol. Immediately before the measurements were started, polyacrylamide chromatography microcolumns were used to exchange the storing buffer for the standard measuring buffer containing 20 mM Tris-HCl (pH 7.4) and 0.2 M NaCl. Steady state absorption spectra were recorded on a Uvikon (Secomam, France) XS UV-vis spectrometer. Photoreduction was carried out in the presence of 10 mM dithiothreitol by continuous light (Intralux6000 lamp from Volpi) passed through a 550 nm long-pass filter (OG550 from Schott).

Time-Resolved Absorption Spectroscopy. Transient absorption changes over 1.6 μs were recorded on a laboratory-built setup essentially as described in ref 17. No external reductant was present during flash experiments. Excitation pulses at 630 nm with a duration of 5 ns provided by a tripled Nd:YAG pumped OPO laser (Rainbow, Quantel, France) were polarized vertically and had an energy of typically 30 mJ/cm². The detection light source was a pulsed Xe arc lamp (FXQ850 from EG&G) equipped with laboratory-built, pulse-forming electronics. The pulses had a duration of several tens of microseconds and a relatively flat top at the beginning of which the excitation pulse was placed. The detection system coupled a FND100Q photodiode (EG&G) to a 30dB, 300 MHz amplifier (HCA, Femto) and the 11A52 plug-in of the DSA602A digitizing oscilloscope (Tektronix) with a 100 MHz bandwidth limit. Traces with and without excitation pulses were recorded in alternating order, typically averaging 32 flashes each. The absorbance changes are calculated as the decadic logarithm of the ratio between the traces with and without excitation. The detection wavelength was chosen by paired interference filters (bandwidth, ~ 10 nm) before the sample and before the detector. To exclude kinetic contributions from depolarization effects after polarized excitation (which under our experimental conditions have a lifetime of ~ 50 ns), we passed the measuring light beam through a sheet polarizer set at the magic angle (54.7°) to the excitation polarization.

The sample was contained in a quartz cell with an optical path length of 10 mm for the measuring beam and 4 mm for the excitation beam. Samples had an absorption of typically 0.15 at 630 nm over 1 cm and were kept at 12 °C. In the course of the transient absorption measurements, samples exhibited some degradation in signal amplitude as established by regular measurements at a reference wavelength (500 nm). Samples were no longer used if this degradation exceeded 30%. Globally fitted signal amplitudes (common lifetime parameters for all studied wavelengths) were corrected for this degradation.

It is of note that in our previous study of wild-type photolyase (8), the measuring light beam was not polarized, and the excitation pulse was largely depolarized by being passed through the wall of the polystyrene cell that was used. The kinetics observed with the more rigorous procedure presented here were virtually indistinguishable from those obtained previously.

Data Processing. Flash-induced absorbance changes (ΔA_λ) at different wavelengths (λ) have then been described by fitting to them globally the following model functions:

$$\Delta A_\lambda(t) = A_\lambda \exp(-t/\tau) + C_\lambda \text{ ("monoexponential fit")} \quad (1)$$

$$\Delta A_{\lambda}(t) = A_{\lambda}[\exp(-t/\tau_1) + B \exp(-t/\tau_2)] + C_{\lambda}$$

(“biexponential fit with a fixed amplitude ratio”) (2)

$$\Delta A_{\lambda}(t) = A_{\lambda} \exp[-(t/\tau)^{\beta}] + C_{\lambda}$$

(“stretched exponential fit”) (3)

Here, τ_i values are global decay time constants. In the amplitude-ratio fixed biexponential fit, it is assumed that the two phases have identical spectra. The λ -independent parameter B represents the constant ratio of the amplitudes of the two phases. The amplitude after complete decay of all exponentials C_{λ} , as a function of wavelength λ , describes the “resting spectrum”. The “initial amplitude”, i.e., the amplitude extrapolated to time zero at wavelength λ , is calculated as $A_{\lambda}(1 + B) + C_{\lambda}$, where B is non-zero only for the biexponential fit.

RESULTS

Figure 1 shows absorption spectra of isolated photolyases both from the wild type and W306F mutant. The very similar spectra prove that also in the mutant *E. coli* photolyase, the flavin cofactor was in the neutral radical state FADH° (absorption bands at 500, 580, and 630 nm), with a tiny portion of oxidized flavin present (absorption band at 450 nm). Photoreduction with >550 nm light was attempted in the presence of 10 mM dithiothreitol as an external reductant. Whereas illumination for 4 min converted the flavin radical largely to the reduced state in the wild type, in the mutant very little reduction occurred (Figure 1, inset), confirming that this mutant is seriously hampered in long-lived photoreduction of the flavin cofactor (12).

In Figures 2 and 3, we compared the flash-induced transient absorption behavior of W306F mutant photolyase with that of the wild type measured in the same setup. For these measurements, no extrinsic reductant was added to prevent accumulation of FADH^{-} during repetitive excitation. Single-wavelength transients like those shown in Figure 2 (590 nm) were recorded between 410 and 670 nm. Both samples exhibited pronounced kinetics in our 1.6 μs time window, the spectral and temporal characteristics being rather different. As reported previously (8), the wild-type sample exhibited an initial absorbance decrease with kinetics faster than the time resolution of our apparatus (10 ns). This absorbance change has been attributed to the formation of FADH^{-} and the cation radical ($\text{TrpH}^{\circ+}$) of W306 [known to be the final intrinsic electron donor in *E. coli* photolyase (12)], as its spectrum [Figure 3A (▼)] is described well as the sum of a $\text{FADH}^{-} - \text{FADH}^{\circ}$ difference spectrum and a $\text{TrpH}^{\circ+} - \text{TrpH}$ difference spectrum (8). In wild-type photolyase, this “initial” spectrum evolved with monoexponential kinetics (time constant of ~ 200 ns) to a “resting” spectrum (stable on the time scale of our experiment). The 200 ns reaction has been assigned to deprotonation of $\text{TrpH}^{\circ+}$, and the resting spectrum [Figure 3A (◆)] has been shown to be described well as a sum of a $\text{FADH}^{-} - \text{FADH}^{\circ}$ difference spectrum and a $\text{Trp}^{\circ} - \text{TrpH}$ difference spectrum (8).

In contrast, in the W306F mutant photolyase sample, the initial absorbance decrease recovered almost completely within the 1.6 μs time window. Global analysis of the traces at all measured wavelengths according to a single-exponential

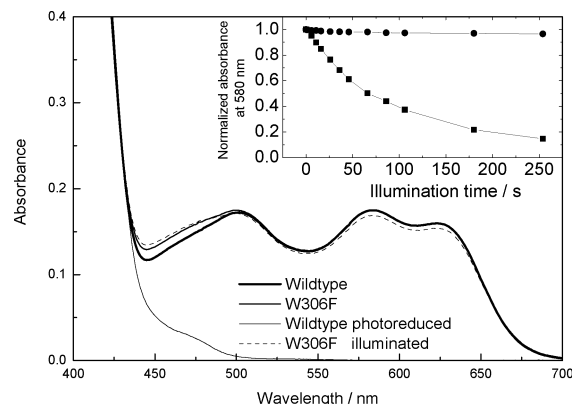


FIGURE 1: Steady state spectra of wild-type and W306F mutant photolyases (normalized at 580 nm) with the flavin in the radical state as well as for wild-type photolyase after complete photoreduction with dithiothreitol (thin line). The inset shows the time course of photoreduction for both W306F mutant (●) and wild-type (■) photolyase as followed by peak absorption at 580 nm. The spectrum of W306F mutant photolyase after illumination for 250 s is shown as a dashed line.

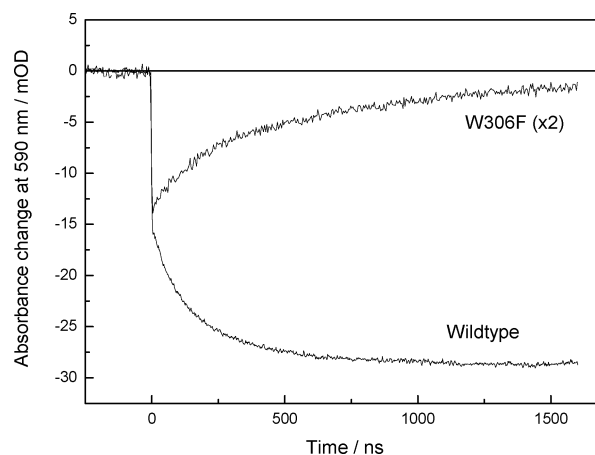


FIGURE 2: Flash-induced transient absorbance changes of wild-type and W306F mutant photolyases at 590 nm. Note that for better comparison the mutant curve was magnified twice.

decay with a constant (accounting for a small resting signal and/or baseline fluctuations) yielded a time constant of 550 ns. The quality of these fits was, however, not satisfying as they did neither describe well a faster contribution at the beginning nor a slower contribution at the end of the fitting window. The decays were better described (see Data Processing in Materials and Methods) by a stretched exponential with a τ of 450 ns and a β of 0.7, and even better by the sum of two exponential phases (time constants $\tau = 99$ and 602 ns at a global amplitude ratio B of 3.4), and a small constant (6% of the total amplitude at 590 nm). The initial spectrum obtained by the latter fit is shown in Figure 3B (■), along with the resting spectrum (●).

In Figure 3, the amplitudes for wild-type and W306F mutant photolyases were rescaled to correct for slight differences in sample concentration and excitation energy and can thus be compared directly. Such comparison reveals that the initial absorbance decrease for W306F mutant photolyase is weaker than for the wild type. At ~ 580 nm, the initial amplitude of the mutant sample was ~ 2 times smaller than that of the wild type and ~ 3.5 times smaller than the wild-type resting amplitude.

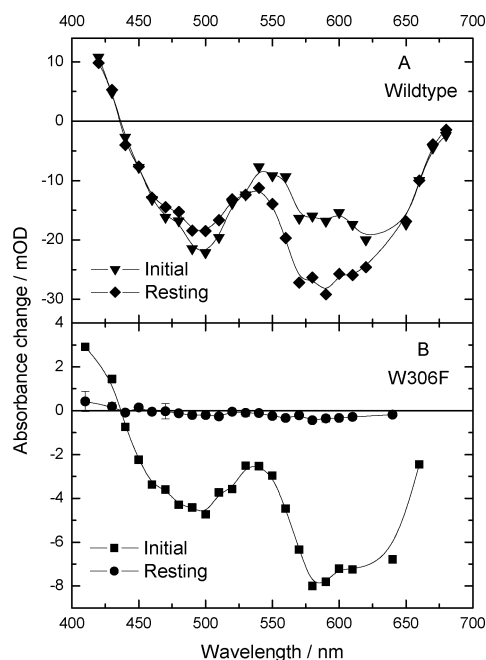


FIGURE 3: Transient spectra of wild-type (A) and W306F mutant (B) photolyases obtained from global fits (wild type, eq 1; W306F, eq 2) to traces as in Figure 2. Initial is the amplitude as extrapolated to time zero, and resting is the constant C_λ found by the fit. Error bars (mostly not surpassing symbol size) were obtained from the corresponding absorption transients (as in Figure 2) by calculating the standard deviation of the noise over the last (quasi-constant) 25 data points.

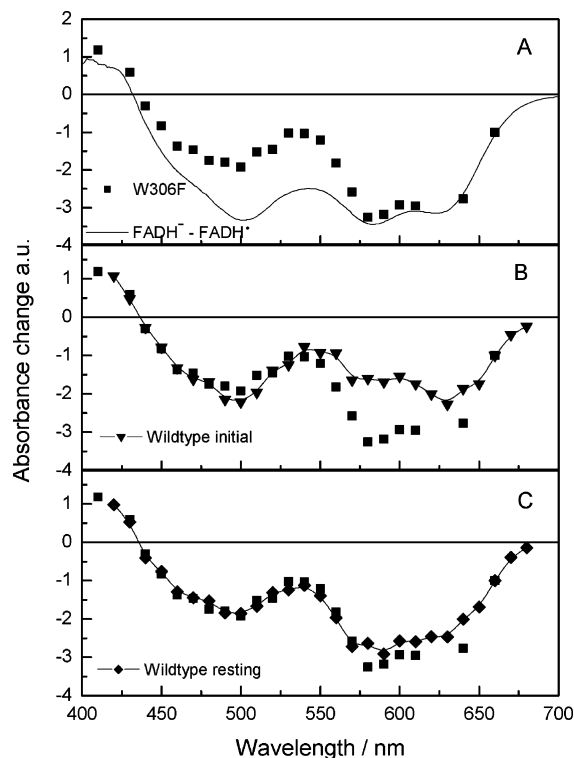


FIGURE 4: Initial transient spectrum of W306F mutant photolyase from Figure 3B (■) compared to the steady state difference spectrum for flavin radical reduction (A) and the two wild-type spectra shown in Figure 3A, all normalized at 660 nm (B and C).

To clarify the nature of the transient state (formed in <10 ns and decaying in $\sim 1 \mu\text{s}$) observed in the W306F mutant, we replot its spectrum in Figure 4 along with three reference spectra of wild-type photolyase: the $\text{FADH}^\bullet - \text{FADH}^+$

difference spectrum as calculated from the traces in Figure 1 (A), the initial spectrum [attributed to formation of $\text{FADH}^\bullet_{306}\text{TrpH}^{+\bullet}$ (B)], and the resting spectrum [attributed to formation of $\text{FADH}^\bullet_{306}\text{Trp}^\circ$ (C)]. Normalization was always in the “flavin-only” region of >650 nm, as described in ref 8. The comparison shows that the initial spectrum of the W306F mutant photolyase sample does definitely not fit to either of the two reference spectra in panel A or B of Figure 4 but is very similar to the resting wild-type spectrum. This accordance suggests that the observed transient state in W306F mutant photolyase has the same chemical nature as the resting state in wild-type photolyase, i.e., a reduced flavin (FADH^\bullet) and neutral (deprotonated) tryptophanyl radical (Trp°). The slight deviation between the two spectra in Figure 4C is discussed below.

DISCUSSION

When our results on the W306F mutant photolyase are compared with those of Li et al. (12), there is a reasonable agreement with respect to the decay kinetics of the transient species. Those authors described it with a first-order rate constant of $\sim 2 \times 10^6 \text{ s}^{-1}$ which is close to our monoexponential fit with a time constant of 550 ns (although we obtained a better fit with two exponentials of 99 and 602 ns). The spectrum of the transient species in the W306F mutant photolyase was not shown in ref 12, yet it was stated that the transient spectrum measured 500 ns after excitation showed “essentially the same general features” as the corresponding spectra of wild-type and W306Y mutant photolyases but was of “lower resolution”. Li et al. (12) attributed all these spectra to the quartet state $^4\text{FADH}^{\circ*}$. The role of $^4\text{FADH}^{\circ*}$ as a long-lived electron-abstracting species was maintained in a recent comprehensive review of photolyase (1).

However, by now it seems well-established that reduction of excited FADH° in wild-type photolyase occurs on a tens of picoseconds time scale (8, 11, 18, 19). W306 is oxidized in less than 10 ns to its cation radical form $\text{TrpH}^{\circ+}$ which releases a proton to bulk water in ~ 200 ns (8). In the absence of W382, the excited flavinyl radical decays in 80 ps to the ground state (9). It is hence clear that the spectrum observed by Li et al. (12) after 500 ns in wild-type photolyase cannot be due to the flavin quartet state, and there is no reason to assume that the spectrum with “essentially the same general features” observed by the same authors in the W306F mutant photolyase should represent the flavin quartet state. Our well-resolved spectral data strongly indicate that the transient species observed in the W306F mutant photolyase has the same chemical nature as the state present in wild-type photolyase after completion of the 200 ns deprotonation reaction, i.e., $\text{FADH}^\bullet\text{Trp}^\circ$. The decay of its transient absorption spectrum to virtually zero in our $1.6 \mu\text{s}$ time window must then be ascribed to a recombination reaction where FADH^\bullet reduces the oxidized tryptophan. The transient oxidation in the W306F mutant photolyase of a tryptophan residue that is definitively not W306 lends strong support to our earlier claim that the intervening tryptophans W359 and W382 located between W306 and the flavin are real intermediates in the electron transfer process along the chain $\text{FADH}^\circ \leftarrow \text{W382} \leftarrow \text{W359} \leftarrow \text{W306}$ in wild-type photolyase.

The slight deviation between the initial spectrum in the W306F mutant photolyase and the resting spectrum in the

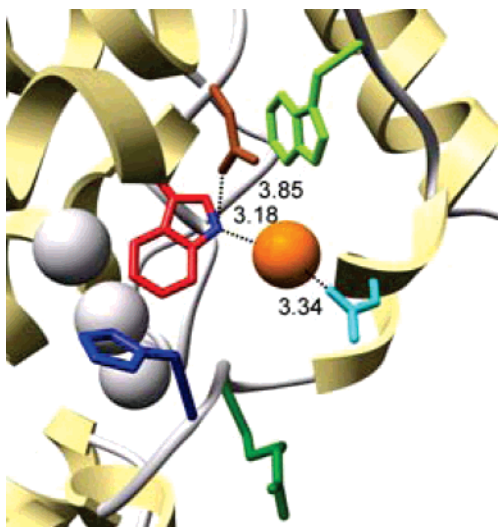


FIGURE 5: Extract from the crystal structure (PDB entry 1dnp, A-chain) of photolyase from *E. coli* (5) showing amino acids H294 (blue), R295 (dark green), D302 (cyan), W306 (light green), D358 (brown), and W359 (red, N1 in blue). Water oxygens situated within 6 Å of W359 are shown as van der Waals spheres, the one closest to NE1 of W359 being highlighted in gold. Distances in angstroms are indicated in black. This figure was prepared with Chimera.

wild type (Figure 4C) is at the limit of the amplitude resolution of our experiments. It might be due to differences in the environments of the contributing oxidized tryptophanyl residues [${}_{306}\text{Trp}^\circ$ in wild-type photolyase and, most likely, ${}_{359}\text{Trp}^\circ$ in the W306F mutant (see below)]. In particular, the electric field exerted by the negative charge of FADH^- should be stronger for ${}_{359}\text{Trp}^\circ$ than for ${}_{306}\text{Trp}^\circ$, and the field orientation with respect to their optical transition moments should be different. Both differences might give rise to slightly different Trp° absorption spectra.

The natural candidates for the location of the tryptophanyl radical living for hundreds of nanoseconds in the W306F mutant photolyase are W382 (proximal to the flavin ring) and W359 (located between W382 and W306 in wild-type photolyase). Spectral data do not allow us to decide between these two chemically identical residues. There are, however, two other arguments in favor of W359.

First, if the radical observed in the W306F mutant photolyase were located on W382, its behavior should be the same or similar to that in the W359F mutant photolyase where the electron transfer chain is interrupted just behind W382. A recent study suggests, however, that the state ($\text{FADH}^-\text{TrpH}^{\circ+}$) of the latter mutant decays by charge recombination in <4 ps, leaving no long-lived photoproducts (10).

Second, as the tryptophanyl radical in the W306F mutant photolyase was deprotonated at the earliest time accessible with our setup (10 ns), there must be a proton acceptor in its proximity. For W382, according to the X-ray structure of wild-type photolyase (5), no potential proton acceptor is present within 4 Å of the N1 nitrogen that carries the dissociable proton. By contrast, for W359, several protonatable groups may be accessed by the N1 proton (Figure 5). First, a water oxygen (colored gold) is found just opposite of N1 of W359 within H-bonding distance (3.2 Å) of it; as the same oxygen is within H-bonding distance (3.3 Å) of a side chain oxygen of D302, a quick proton relay may be assured. A side chain oxygen of D358 is also within H-bonding distance of N1 of W359, but the putative $\text{N}-\text{H}\cdots\text{O}$ angle is rather

too small for a H-bond. Finally, there might be other ways for a proton to migrate in the vicinity of W359 as this residue and H294 form a cleft that harbors at least three water molecules in good contact among each other and other amino acids.

The recombination reaction between FADH^- and the deprotonated tryptophanyl radical (most likely ${}_{359}\text{Trp}^\circ$) in the W306F mutant photolyase occurred on a time scale of hundreds of nanoseconds and required at least two exponential phases ($\tau = 99$ and 602 ns) for an adequate description [the small resting spectrum similar in shape to the initial spectrum (Figure 3B) points to the existence of an additional, slower component of the same recombination]. Obviously, this recombination must include reprotonation of the tryptophan, in addition to back electron transfer. According to a semiempirical rule for the distance dependence of intraprotein electron transfer (20), transfer of an electron from FADH^- to ${}_{359}\text{TrpH}^{\circ+}$ (edge-to-edge distance, 10 Å) could be as fast as ≈ 1 ns (optimal case when the driving force matches the reorganization energy); it might be even faster if it involved repopulation of ${}_{382}\text{TrpH}^{\circ+}$. We attribute the observed much slower recombination kinetics to the preceding reprotonation process [though, at present, we cannot exclude the possibility of a concerted proton-coupled electron transfer (PCET) reaction]. Reprotonation of ${}_{359}\text{Trp}^\circ$ might be the rate-limiting step of the recombination, or if reprotonation is fast, the effective recombination may be slowed due to a small population of ${}_{359}\text{TrpH}^{\circ+}$ in quasi-equilibrium with ${}_{359}\text{Trp}^\circ$, similar to the mechanism suggested for the recombination between FADH^- and ${}_{306}\text{Trp}^\circ$ in wild-type photolyase (21). As W359 appears to be part of a multiple-site proton network (see above), reprotonation of ${}_{359}\text{Trp}^\circ$ might be kinetically complex and give rise to the observed multiexponential recombination kinetics in the W306F mutant photolyase. Noteworthy is the fact that the change in pH from 7.4 to 6.0 (MES buffer) did not affect the recombination kinetics in W306F mutant photolyase (not shown). This is in contrast to wild-type photolyase, where the recombination between FADH^- and ${}_{306}\text{Trp}^\circ$ accelerated more than 7-fold with the same pH change, in line with a good accessibility of N1 of W306 to the bulk solution (21). We conclude that the proton released from ${}_{359}\text{TrpH}^{\circ+}$ in the W306F mutant photolyase does not escape to the bulk solution but rather remains in the protein interior during the lifetime of the state ($\text{FADH}^-\text{}_{359}\text{Trp}^\circ$).

We were not able to monitor the deprotonation of ${}_{359}\text{TrpH}^{\circ+}$ at our setup's time resolution of 10 ns and conclude that the deprotonation has to be faster. It could even be concerted with the electron transfer. In this context, it is interesting that the yield of formation of the state ($\text{FADH}^-\text{}_{359}\text{Trp}^\circ$) in the W306F mutant photolyase was ~ 3.5 times smaller than that of ($\text{FADH}^-\text{}_{306}\text{Trp}^\circ$) in the wild type. A straightforward explanation would be unfavorable competition between deprotonation of ${}_{359}\text{TrpH}^{\circ+}$ and back electron transfer from FADH^- to ${}_{359}\text{TrpH}^{\circ+}$ in the mutant, while in wild-type photolyase, transfer of an electron from ${}_{306}\text{TrpH}$ to ${}_{359}\text{TrpH}^{\circ+}$ is faster than back electron transfer from FADH^- and also faster than deprotonation of ${}_{359}\text{TrpH}^{\circ+}$ (otherwise, formation of ${}_{359}\text{Trp}^\circ$ might severely slow or block the oxidation of ${}_{306}\text{TrpH}^{\circ+}$). To resolve these processes, we are currently preparing an improvement in the time resolution of our transient absorption setup.

ACKNOWLEDGMENT

We thank Dr. M. Modesti for valuable help in preparing the mutant photolyase gene, Drs. A. Yasui and K. Yamamoto for providing us with the pKE plasmid and *E. coli* KY29 strain, respectively, and Dr. J. H. J. Hoeijmakers for his continuous interest in this project.

REFERENCES

1. Sancar, A. (2003) Structure and function of DNA photolyase and cryptochrome blue-light photoreceptors, *Chem. Rev.* 103, 2203–2237.
2. Weber, S. (2005) Light-driven enzymatic catalysis of DNA repair: A review of recent biophysical studies on photolyase, *Biochim. Biophys. Acta* 1707, 1–23.
3. Kavakli, I. H., and Sancar, A. (2004) Analysis of the role of intraprotein electron transfer in photoreactivation by DNA photolyase in vivo, *Biochemistry* 43, 15103–15110.
4. Kim, S. T., Heelis, P. F., and Sancar, A. (1995) Role of tryptophans in substrate binding and catalysis by DNA photolyase, *Methods Enzymol.* 258, 319–343.
5. Park, H. W., Kim, S. T., Sancar, A., and Deisenhofer, J. (1995) Crystal structure of DNA photolyase from *Escherichia coli*, *Science* 268, 1866–1872.
6. Heelis, P. F., Payne, G., and Sancar, A. (1987) Photochemical properties of *Escherichia coli* DNA photolyase: Selective photodecomposition of the second chromophore, *Biochemistry* 26, 4634–4640.
7. Cheung, M. S., Daizadeh, I., Stuchebrukhov, A. A., and Heelis, P. F. (1999) Pathways of electron transfer in *Escherichia coli* DNA photolyase: Trp306 to FADH, *Biophys. J.* 76, 1241–1249.
8. Aubert, C., Vos, M. H., Mathis, P., Eker, A. P. M., and Brettel, K. (2000) Intraprotein radical transfer during photoactivation of DNA photolyase, *Nature* 405, 586–590.
9. Byrdin, M., Eker, A. P. M., Vos, M. H., and Brettel, K. (2003) Dissection of the triple tryptophan electron transfer chain in *Escherichia coli* DNA photolyase: Trp382 is the primary donor in photoactivation, *Proc. Natl. Acad. Sci. U.S.A.* 100, 8676–8681.
10. Lukacs, A., Eker, A. P. M., Byrdin, M., Villette, S., Pan, J., Brettel, K., and Vos, M. H. (2006) Role of the Middle Residue in the Triple Tryptophan Electron Transfer Chain of DNA Photolyase: Ultrafast Spectroscopy of a Trp → Phe Mutant, *J. Phys. Chem. B* 110, 15654–15658.
11. Wang, H., Saxena, C., Quan, D., Sancar, A., and Zhong, D. (2005) Femtosecond Dynamics of Flavin Cofactor in DNA Photolyase: Radical Reduction, Local Solvation, and Charge Recombination, *J. Phys. Chem. B* 109, 1329–1333.
12. Li, Y. F., Heelis, P. F., and Sancar, A. (1991) Active site of DNA photolyase: Tryptophan-306 is the intrinsic hydrogen atom donor essential for flavin radical photoreduction and DNA repair in vitro, *Biochemistry* 30, 6322–6329.
13. Takao, M., Oikawa, A., Eker, A. P. M., and Yasui, A. (1989) Expression of an *Anacystis nidulans* photolyase gene in *Escherichia coli*: Functional complementation and modified action spectrum of photoreactivation, *Photochem. Photobiol.* 50, 633–637.
14. Nakajima, S., Sugiyama, M., Iwai, S., Hitomi, K., Otoshi, E., Kim, S. T., Jiang, C. Z., Todo, T., Britt, A. B., and Yamamoto, K. (1998) Cloning and characterization of a gene (UVR3) required for photorepair of 6-4 photoproducts in *Arabidopsis thaliana*, *Nucleic Acids Res.* 26, 638–644.
15. Akasaka, S., and Yamamoto, K. (1991) Construction of *Escherichia coli* K12 phr deletion and insertion mutants by gene replacement, *Mutat. Res.* 254, 27–35.
16. Eker, A. P. M., Yajima, H., and Yasui, A. (1994) DNA photolyase from the fungus *Neurospora crassa*. Purification, characterization and comparison with other photolyases, *Photochem. Photobiol.* 60, 125–133.
17. Brettel, K., Leibl, W., and Liebl, U. (1998) Electron transfer in the heliobacterial reaction center: Evidence against a quinone-type electron acceptor functioning analogous to A1 in photosystem I, *Biochim. Biophys. Acta* 1363, 175–181.
18. MacFarlane, A. W., and Stanley, R. J. (2003) *Cis-Syn* Thymidine Dimer Repair by DNA Photolyase in Real Time, *Biochemistry* 42, 8558–8568.
19. Saxena, C., Sancar, A., and Zhong, D. (2004) Femtosecond Dynamics of DNA Photolyase: Energy Transfer of Antenna Initiation and Electron Transfer of Cofactor Reduction, *J. Phys. Chem. B* 108, 18026–18033.
20. Page, C. C., Moser, C. C., Chen, X., and Dutton, P. L. (1999) Natural engineering principles of electron tunnelling in biological oxidation-reduction, *Nature* 402, 47–52.
21. Byrdin, M., Sartor, V., Eker, A. P. M., Vos, M. H., Aubert, C., Brettel, K., and Mathis, P. (2004) Intraprotein electron transfer and proton dynamics during photoactivation of DNA photolyase from *E. coli*: Review and new insights from an “inverse” deuterium isotope effect, *Biochim. Biophys. Acta* 1655, 64–70.

BI700891F